International Journal of Design & Nature and Ecodynamics
Vol. 21, No. 6, June, 2026, pp. 1739-1746
Journal homepage: http://iieta.org/journals/ijdne

Green Synthesis of Silver Nanoparticles Using *Pomegranate Peel* Extract: Structural Analysis and Antibacterial Activity Against *Staphylococcus aureus* and *Candida albicans*

Hussein A. Jamil[1*], Nagham K. Jaber[1], Hamza J. Jabour[1], Hala A. Rasheed[2], Shahad S. Khudiar[2]

[1] Department of Biology, College of Science, Mustansiriyah University, Baghdad 10052, Iraq
[2] Department of Physics, College of Science, Mustansiriyah University, Baghdad 10052, Iraq

Corresponding Author Email: Hussein.A.Jamil@uomustansiriyah.edu.iq

https://doi.org/10.18280/ijdne.210618

Received: 17 April 2026
Revised: 8 June 2026
Accepted: 20 June 2026
Available online: 30 June 2026

Keywords:
green synthesis, silver nanoparticles, Punica granatum, antimicrobial activity, Staphylococcus aureus, Candida albicans, nanobiotechnology

ABSTRACT

Silver nanoparticles (AgNPs) were synthesized using aqueous peel extract of *Punica granatum* through an environmentally sustainable green synthesis approach. The synthesized nanoparticles were characterized using UV-Visible spectroscopy, Fourier-transform infrared spectroscopy (FTIR), transmission electron microscopy (TEM), and X-ray diffraction (XRD) analyses. The antimicrobial activity of the synthesized AgNPs was evaluated against clinical isolates of *Staphylococcus aureus* and *Candida albicans* using agar disc diffusion and broth microdilution methods. UV-Visible spectrophotometric analysis revealed a characteristic surface plasmon resonance (SPR) peak at 425–430 nm, confirming nanoparticle formation, while FTIR analysis identified hydroxyl, carbonyl, and amide functional groups potentially involved in silver ion reduction and nanoparticle stabilization. TEM analysis demonstrated predominantly spherical and uniformly distributed nanoparticles. The AgNPs exhibited higher inhibition zones against *S. aureus* (18.6 ± 2.1 mm) and *C. albicans* (17.2 ± 1.8 mm) compared with crude pomegranate peel extract and silver nitrate controls. Minimum inhibitory concentration (MIC) values ranged from 8–32 µg/mL for *S. aureus* and 16–64 µg/mL for *C. albicans*. These findings indicate that pomegranate peel-mediated AgNPs represent promising preliminary eco-friendly antimicrobial candidates. However, long-term storage stability, including changes in particle size, zeta potential, and antimicrobial activity over time, as well as biosafety evaluation, should be investigated in future studies before broader biomedical or formulation-related applications.

1. INTRODUCTION

Bacterial and fungal infections are among the biggest health problems facing the world in the 21st century due to the emergence of new resistant strains. With the continuous increase in resistance to traditional antibiotics and antifungals, this problem leads to decreased treatment effectiveness, increased infection rates, and sometimes even death. Antibiotic resistance rates are rising, particularly among immunocompromised patients and hospitalized patients. According to the WHO, antibiotic resistance has become a serious threat to the world, which requires new therapeutic methods [1, 2]. As a result, there is a critical requirement for environmentally sustainable antimicrobial agents capable of overcoming multidrug resistance.

Staphylococcus aureus is among the most clinically significant bacterial pathogens associated with skin, wound, bloodstream, and respiratory infections. However, the issue of combating *Staphylococcus aureus* is complicated due to the possibility of resistance development in strains. Methicillin-resistant *Staphylococcus aureus* strains have multi-resistance properties and need proper treatment [3, 4]. At the same time, *Candida albicans* is an opportunistic fungus, which is a part of the normal flora in the gut microflora and turns into a pathogen in immunocompromised individuals or due to antibiotic treatment. The increase in the number of hospital-acquired candidiasis cases has been noted in conjunction with increasing antifungal resistance to first-line drugs, fluconazole, and amphotericin B [5, 6].

Recent research has increasingly focused on the application of natural compounds in the search for new therapy approaches, along with the application of nanotechnology. These nanoparticles have many physical and chemical properties, which make them superior to existing antimicrobial techniques; one such property is a large surface area [7]. There were different materials employed as nanoparticles, but silver nanoparticles (AgNPs) have gained much interest due to their vast spectrum of action against Gram-positive and Gram-negative bacteria, fungi, and viruses. Several modes of action of AgNPs as antibacterial agents include destruction of the cell wall, oxidative stress, enzyme inhibition, and interference with DNA [8, 9]. Despite the promising results of AgNPs in curing diseases caused by microbes, the conventional chemical and physical methods for preparing AgNPs might have negative effects on the environment and even be toxic. Thus, a green method was suggested for creating AgNPs employing natural

extracts from plants [10].

Green synthetic methodologies have been developed to ensure that there will not be any kind of hazards to health and promote environmental sustainability. One such example of a medicinal plant utilized extensively in various forms of traditional medicine is pomegranate (*Punica granatum*). The presence of phenolic compounds, flavonoids, tannins, and ellagic acid makes the pomegranate peel antibacterial, antifungal, and antioxidant in nature [11]. Pomegranate peel extract is very capable of suppressing the growth of *Staphylococcus aureus* and *Candida albicans.* Moreover, phytochemicals act as natural reducers during the synthesis of AgNPs and increase biological activity along with decreasing toxicity [12]. Integration of all these medicinal qualities present in pomegranate peel with the broad range of activity exhibited by AgNPs can be taken as a very reliable route towards the synthesis of strong antimicrobials. Antibiotic-resistant bacteria and opportunistic fungi pose a big challenge as far as the use of biofilm is concerned, as it prevents their penetration into the target cells. Biofilms are physically and chemically impermeable barriers that make the standard therapeutic treatment ineffective [13]. AgNPs possess enhanced biofilm penetration ability due to their nanoscale dimensions and large surface-area-to-volume ratio [8, 10]. Although various studies have indicated the antimicrobial properties of AgNPs, limited data are available regarding the green synthesis of AgNPs utilizing pomegranate peel extract against clinically isolated strains from infected wounds in Iraq. The utilization of agricultural waste materials, such as pomegranate peel, contributes to circular bioeconomy strategies and sustainable nanomaterial production.

This study assessed the antibacterial and antifungal properties of eco-friendly AgNPs obtained from the extract of pomegranate peel against *S. aureus* and *C. albicans*.

2. MATERIALS AND METHODS

2.1 Ethical approval and participant information

Ethical approval was obtained from the Institutional Research Ethics Committee of Mustansiriyah University, Baghdad, Iraq (Approval No.: BCSMU/1025/00092Z; approved on December 1, 2025). Fifty clinical specimens were collected from patients with wounds and foot lesions in the surgical and outpatient departments. All participants signed informed consent forms before specimen collection. Specimen collection procedures strictly adhered to sterile surgical technique.

2.2 Clinical isolation and *Candida* species identification

Clinical specimens were collected from the depths of the lesions by vigorously swabbing them with sterile cotton swabs after cleaning their surface with sterile normal saline (0.9%) [14]. The swabs were then cultured on Sabouraud Dextrose Agar (SDA) plates supplemented with chloramphenicol (0.05 g/L) and incubated aerobically for 24–72 hours at 37 °C [15]. This was followed by a preliminary diagnosis, which involved microscopic examination of creamy, paste-like, whitish or off-white colonies using Gram staining to detect Gram-positive (in terms of staining) budding yeast-like fungal cells and the formation of pseudohyphae. *Candida albicans* was differentiated from other *Candida* species utilizing the germ tube test (incubation in human serum for 3 hours at 37 °C) and chlamydial spore formation on corn flour agar (CMA) containing Tween 80 at 25–28 °C. Diagnosis was then made employing the CHROMagar™ Candida plate for rapid species identification based on colony color differentiation (green for *Candida albicans*) [16].

2.3 Clinical isolation and identification of *Staphylococcus aureus*

Clinical swabs were cultured on blood agar and mannitol salt agar (MSA) plates for 24–48 hours at 37 °C. Strains exhibiting golden-yellow colonies with fermentative activity (yellow areas) were isolated utilizing MSA plates. The isolates were identified as Gram-positive cocci arranged in grape-like clusters employing microscopic analysis. Bacterial isolation was confirmed by biochemical tests, specifically catalase and coagulase assays [17].

2.4 Preparation of Pomegranate Peel Extract

Aqueous extraction was performed employing fresh pomegranate (*Punica granatum*) peels. The peels were cleaned with deionized water, allowed to air-dry at room temperature, and ground into a fine powder. To prepare 10% (w/v) aqueous extract, 10 g of the powder was dissolved in 100 mL of distilled water. The mixture was stirred for 30 minutes in a magnetic stirrer at a temperature of 60-70 °C. The extract was then filtered employing Whatman No. 1 filter paper and stored at a temperature of 4 °C to minimize microbial contamination and reduce phytochemical degradation prior to nanoparticle synthesis [18].

2.5 Biosynthesis and isolation of silver nanoparticles

Biosynthesis was performed by mixing pomegranate peel extract with a 1 mM silver nitrate ($AgNO_3$) solution (1:9 v/v). The reactions were carried out in complete darkness at room temperature for 24 hours to avoid photoreduction. The reduction of silver ions (Ag^+) to silver atoms (Ag^0) was observed by a color change from colorless to dark brown. The isolated nanoparticles were centrifuged (10,000 rpm for 15 minutes), washed three times with distilled water to remove any remaining metabolites, and then freeze-dried [19].

2.6 Characterization of the silver nanoparticles

Elemental composition analysis by EDX was not performed in this study. Therefore, nanoparticle characterization was based on UV–Vis, FTIR, TEM, XRD, and zeta potential analyses.

A) Ultraviolet-visible (UV-Vis): UV-Vis spectroscopy was employed to determine the spectral properties of the nanoparticles in the 300–800 nm range using a Shimadzu spectrometer (Japan) [20].

B) Fourier transform infrared spectroscopy (FTIR): Functional groups responsible for encapsulating and stabilizing the nanoparticles were identified employing FTIR spectroscopy (Brücker, Germany) in the 400–4000 cm^{-1} range [21].

C) Transmission electron microscopy (TEM): TEM was performed to study the morphological and crystalline structure of the AgNPs [22]. TEM analysis was performed employing a JEOL JEM-2100 microscope operated at 200 kV. Samples

were prepared by depositing a drop of AgNP suspension onto carbon-coated copper grids, followed by air drying. Particle size analysis was performed utilizing images obtained at magnifications ranging from × 50,000 to × 150,000. Particle size distribution was determined from calibrated TEM micrographs using image-analysis software. A total of 42 clearly distinguishable nanoparticles were measured as a representative TEM-based size analysis. Adjacent particles with visible boundaries were included, whereas severely agglomerated, merged, or unclear particles were excluded to minimize measurement bias and avoid overestimation of particle diameter. The TEM-derived size dispersion index was calculated using the equation PDI = (SD/mean particle size)².

D) X-ray diffraction (XRD): XRD analysis was carried out to assess the crystalline nature and phase composition of the synthesized AgNPs. The XRD pattern was recorded using Cu Kα radiation (λ = 1.5406 Å) over a 2θ range of 20°–80°, at a scan rate of 2° min^{-1} and a step size of 0.02° [23].

E) Zeta potential analysis: Zeta potential was measured to evaluate the initial surface charge and colloidal stability tendency of the synthesized AgNP suspension at the time of characterization.

2.7 Antimicrobial bioassay

Antimicrobial potential was assessed using the disc diffusion technique. A suspension of standard microorganisms (1.5×10^8 CFU/ml for bacteria and 1×10^6 cells/ml for yeast; McFarland 0.5) was spread onto Mueller-Hinton agar (for *Staphylococcus aureus*) and SDA agar for *Candida albicans*. Sterile filter paper discs were impregnated with synthesized AgNPs, crude PPE extract, silver nitrate, and distilled water, as a control. Vancomycin and fluconazole were employed as positive controls for bacterial and fungal assays, respectively. The area of inhibition was then independently measured (in millimeters) by two blinded investigators after an incubation period of 24–48 hours [24]. All experiments were conducted in triplicate under identical laboratory conditions.

2.8 Determination of antimicrobial activity

The minimum inhibitory concentration (MIC) values were determined employing a broth microdilution assay in 96-well plates according to the Clinical and Laboratory Standards Institute (CLSI) guidelines. A bifold sequential dilution series of the synthesized AgNPs (0.5–256 µg/mL) was performed in Mueller-Hinton broth for *Staphylococcus aureus* and RPMI-1640 medium for *Candida albicans*. The minimum bactericidal concentration (MBC) and minimum fungicidal concentration (MFC) of the samples were obtained by re-seeding the transparent wells onto an agar plate [25].

2.9 Statistical analysis

Each experiment was carried out in three replicates (n = 3). Values are presented as mean ± standard deviation (SD). Data significance was calculated employing one-way ANOVA, followed by Tukey's test. In all experiments, a p-value < 0.05 was considered statistically significant. All statistical tests were performed utilizing the Statistical Package for the SPSS version 27 (IBM Corp., USA).

3. RESULTS AND DISCUSSION

3.1 Evaluation of silver nanoparticles produced from pomegranate peels

AgNPs were produced using pomegranate peel extract through an environmentally friendly green synthesis approach. The formation process was initially indicated by a characteristic color change from transparent to dark brown, suggesting the reduction of silver ions (Ag^+) into AgNPs. Such a color transformation represents a reliable preliminary optical indicator supporting AgNP biosynthesis and agrees with previous observations describing brownish coloration as a distinctive feature of AgNP formation [26, 27].

The formation of AgNPs was further supported by UV–Vis absorption spectroscopy, which revealed a characteristic absorption peak at 425–430 nm corresponding to the surface plasmon resonance (SPR) of AgNPs, as shown in Figure 1. This observation provides important information regarding nanoparticle formation, dispersion, and possible aggregation behavior. The sharp SPR peak suggests relatively uniform particle distribution under the initial characterization conditions, while storage-dependent stability requires further time-course evaluation.

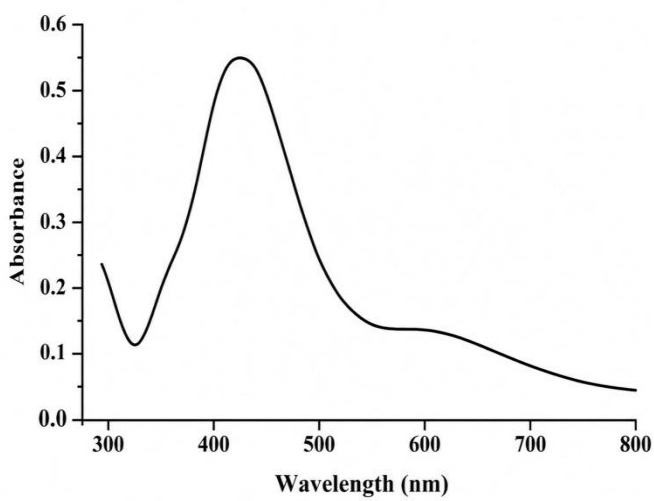

Figure 1. UV–Vis absorption spectrum of the synthesized AgNPs showing the characteristic surface plasmon resonance (SPR) peak at 425–430 nm

FTIR analysis was performed to identify the biomolecular functional groups potentially involved in the reduction and surface stabilization of the synthesized AgNPs. The FTIR peak at 3450.65 cm^{-1} corresponds to the hydroxyl (-OH) stretching vibrations from phenolic compounds, suggesting their primary involvement in Ag^+ reduction and nanoparticle stabilization. Significant peaks were also observed at 1653.00 cm^{-1} and 1560.41 cm^{-1}, which are characteristic of carbonyl (C=O) and amide (-NH) functional groups, respectively. Additionally, the peak at 1473.62 cm^{-1} and the fingerprint region peak at 1066.64 cm^{-1} further indicate the presence of proteins and polyols. These functional groups contribute to the effective reduction, capping, and long-term stabilization of the biologically synthesized AgNPs, as illustrated in Figure 2.

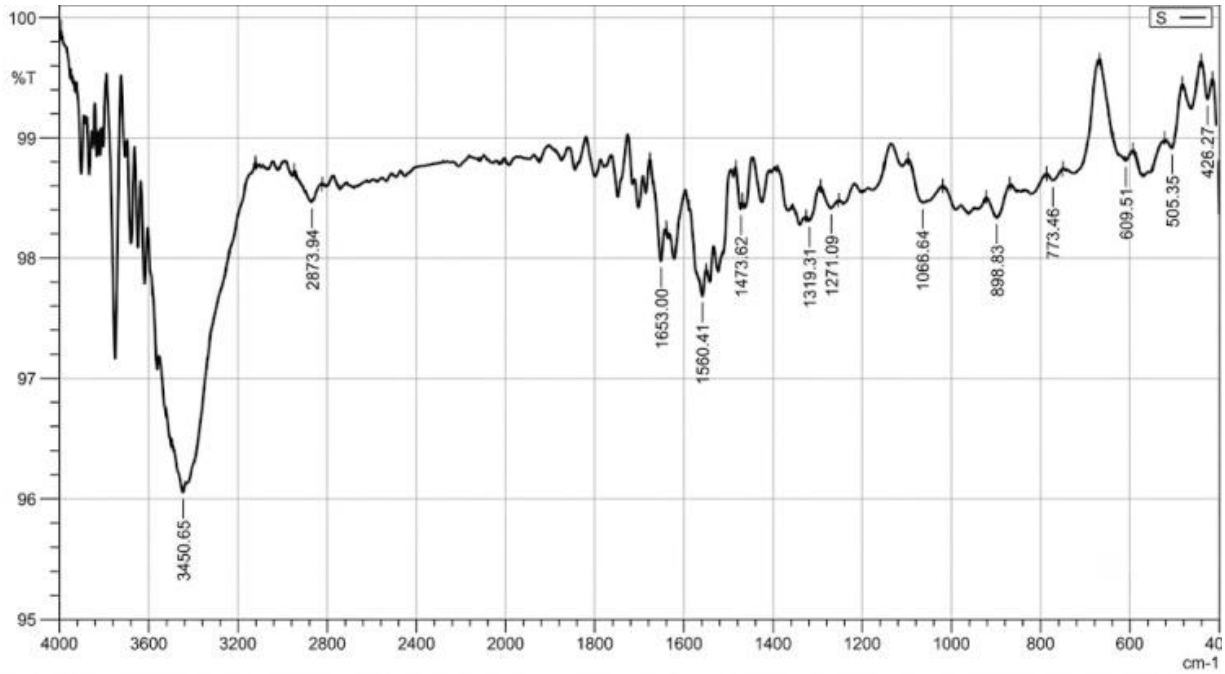

Figure 2. Fourier transform infrared spectroscopy (FTIR) spectrum of the biologically synthesized AgNPs, highlighting the key biomolecular functional groups involved in reduction and surface stabilization

TEM analysis revealed that the synthesized AgNPs were predominantly spherical to nearly spherical, with partial agglomeration observed in some regions of the micrograph. TEM-based particle size distribution analysis showed that the nanoparticles were distributed within the range of 20–80 nm. Based on the measurement of 42 clearly distinguishable particles from calibrated TEM micrographs, the mean particle size was 42.6 ± 17.0 nm. The TEM-derived polydispersity index, calculated as PDI = (SD/mean particle size)², was 0.159. The corresponding particle size histogram showed that most particles were distributed within the 20–50 nm range, representing approximately 71.4% of the measured particles, as shown in Figure 3. These findings indicate that the synthesized AgNPs were mainly nanosized, with moderate particle-size dispersion.

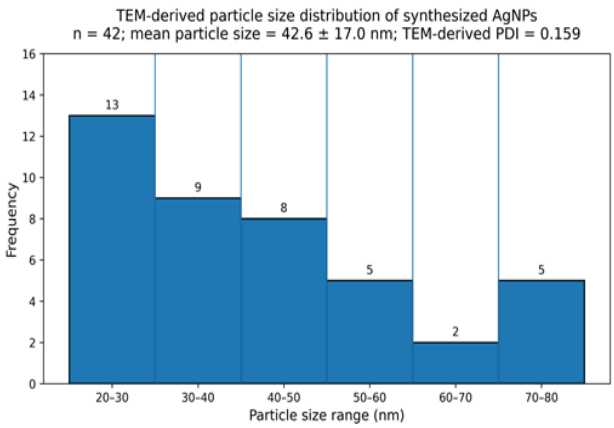

Figure 3. Transmission electron microscopy (TEM)-derived particle size distribution of the synthesized AgNPs

Notes: The histogram was generated from 42 clearly distinguishable nanoparticles measured from calibrated TEM micrographs. The measured particles showed a size range of 20–80 nm, with a mean particle size of 42.6 ± 17.0 nm and a TEM-derived PDI of 0.159. Most measured particles were distributed within the 20–50 nm range.

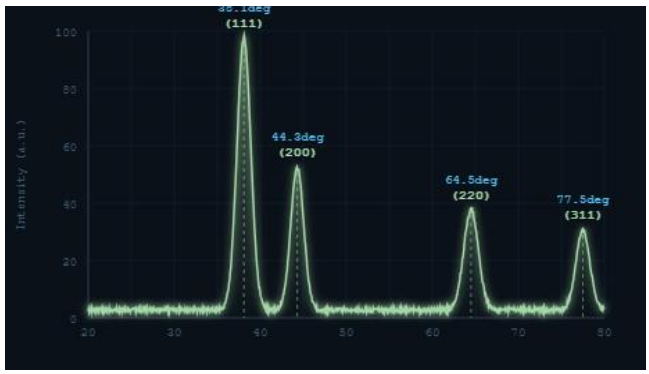

Figure 4. X-ray diffraction (XRD) pattern of the synthesized AgNPs showing the characteristic diffraction peaks of face-centered cubic silver at the (111), (200), (220), and (311) crystalline planes

Table 1. Physicochemical characterization of green-synthesized silver nanoparticles (AgNPs)

Characterization Technique	Parameter	Observation/Values
Visual Inspection	Color Transition	Colorless to dark brown
UV-Vis Spectroscopy	SPR Peak	425–430 nm
FTIR Spectroscopy	Key Functional Groups	–OH, C=O, –NH, C–N
TEM Analysis	Particle size distribution	20–80 nm; mean = 42.6 ± 17.0 nm; n = 42; TEM-derived PDI = 0.159
XRD Analysis	Crystal Structure	FCC (111, 200, 220, 311)
Zeta Potential Analysis	Initial surface charge at the time of characterization	-25 to -30 mV

Notes: FTIR: Fourier transform infrared spectroscopy; TEM: Transmission electron microscopy; XRD: X-ray diffraction.

XRD analysis showed characteristic diffraction peaks corresponding to the face-centered cubic structure of metallic silver, including the (111), (200), (220), and (311) crystalline planes, as shown in Figure 4. These peaks support the crystalline nature and phase composition of the synthesized AgNPs.

The measured zeta potential value of -25 to -30 mV indicates initial electrostatic stabilization of the nanoparticle suspension at the time of analysis. However, storage-dependent changes in zeta potential were not assessed in the present study.

The main physicochemical characterization findings of the green-synthesized AgNPs, including visual color change, UV–Vis SPR peak, FTIR functional groups, TEM-derived particle size distribution, zeta potential, and XRD crystalline structure, are summarized in Table 1.

3.2 Antimicrobial potential of silver nanoparticles against *Staphylococcus aureus* and *Candida albicans*

Table 2. Inhibition zones of various treatments against *Staphylococcus aureus* and *Candida albicans*

Treatment Groups	Concentration/ Volume	Zone of Inhibition (mm) Against S. *aureus*	Zone of Inhibition (mm) Against *C. Albicans*
Synthesized AgNPs	Optimized	18.6 ± 2.1	17.2 ± 1.8
Pomegranate extract (PPE)	10% (w/v)	10.2 ± 1.4	9.6 ± 1.2
Silver nitrate ($AgNO_3$)	1 mM	12.5 ± 1.6	11.8 ± 1.5
Distilled water (-ve control)	100 µL	0.0	0.0

Notes: -ve control: Negative control (distilled water).

The disc diffusion assay was employed to assess the antibacterial potential of AgNPs against Staphylococcus aureus. In this regard, the inhibition zone appeared to be clear with an average value of the diameter of 18.6 ± 2.1 mm, which is significantly higher compared to that of crude pomegranate peel extract (10.2 ± 1.4 mm) and silver nitrate solution (12.5 ± 1.6 mm). In turn, the absence of activity for distilled water shows that the antibacterial potential is a consequence of the utilization of the specific nanoparticles or extracts [28, 29]. At the same time, it should be noted that the antimicrobial potential of AgNPs is concentration-dependent, as the antimicrobial potential increased with increasing concentrations of the nanoparticles. This finding confirms the concentration dependency of the activity under analysis. Several studies have reported multiple mechanisms of the antibacterial effect of the nanoparticles, including damaging cell walls, inducing oxidative stress, interfering with key enzymes, and penetrating into DNA, which leads to death or growth inhibition [30]. Meanwhile, in terms of fungi, AgNPs demonstrated effective antifungal potential against Candida albicans with the inhibition zone diameter averaging 17.2 ± 1.8 mm. The successful inhibition of the growth of *S. aureus* and *C. albicans* by AgNPs implies the applicability of such nanotechnology in designing new or complementary therapies of natural origin amid increasing cases of resistance to drugs. The observed enhanced efficacy may be associated with the increased surface-area-to-volume ratio and improved interaction between AgNPs and microbial cell membranes. The lower MIC values obtained for *S. aureus* compared with *C. albicans* suggest that bacterial cells were more susceptible to AgNP treatment than fungal cells. It was revealed in earlier studies that AgNPs synthesized from plants proved to be extremely efficient against different pathogens. Moreover, biosynthesis based on the use of plant extract is regarded as an environmentally friendly and non-toxic process [15]. Table 2 and Figure 5 show the antimicrobial efficacy (inhibition zone in mm ± SD) of AgNPs, pomegranate peel extract, and controls against *Staphylococcus aureus* and *Candida albicans*.

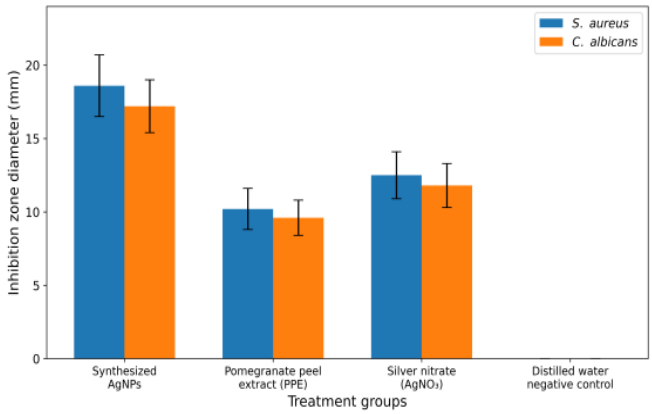

Figure 5. Antimicrobial activity of green-synthesized AgNPs, pomegranate peel extract (PPE), silver nitrate ($AgNO_3$), and distilled water as a negative control against *Staphylococcus aureus* and *Candida albicans*

Notes: Bars represent the mean inhibition zone diameter (mm), and error bars indicate the standard deviation (SD) of triplicate measurements (n = 3). Statistical differences among treatment groups were analyzed using one-way ANOVA followed by Tukey's post hoc test, with $p < 0.05$ considered statistically significant.

3.3 Minimum inhibitory concentration, minimum bactericidal concentration, and minimum fungicidal concentration of silver nanoparticles synthesized with pomegranate peel extract

Table 3 and Figure 6 demonstrated that the obtained results from the broth microdilution technique revealed the very high efficiency of the AgNPs synthesized with the help of pomegranate peel extract in inhibiting *S. aureus* growth, with the MIC value being in the range of 8-32 µg/mL and the MBC value of 16-64 µg/mL. The results demonstrated that AgNPs possess dual functionalities, since they not only inhibit the growth but also eliminate bacteria. For the *C. albicans* strain, the MIC value was found to be between 16 and 64 µg/mL, and the MFC was between 32 and 128 µg/mL.

Table 3. MIC and MBC/MFC ranges of green-synthesized silver nanoparticles (AgNPs) against *Staphylococcus aureus* and *Candida albicans*

Microorganism	MIC (µg/mL)	MBC / MFC (µg/mL)
Staphylococcus aureus	8–32	16–64
Candida albicans	16–64	32–128

Notes: MIC: Minimum inhibitory concentration; MBC: Minimum bactericidal concentration; MFC: Minimum fungicidal concentration. Values represent the concentration ranges obtained from the broth microdilution assay under in vitro conditions.

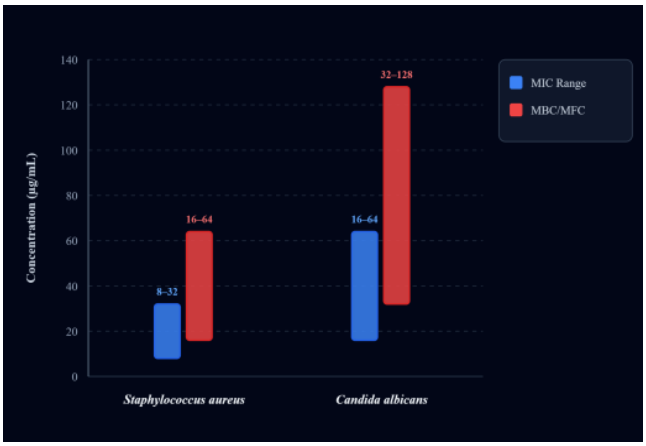

Figure 6. Initial in vitro MIC and MBC/MFC ranges of biosynthesized silver nanoparticles (AgNPs) against *Staphylococcus aureus* and *Candida albicans*
Notes: MIC: Minimum inhibitory concentration; MBC: Minimum bactericidal concentration; MFC: Minimum fungicidal concentration.

Thus, it is possible to state that the biosynthesis of AgNPs through the utilization of pomegranate peel extract has a high correlation with several studies showing the efficiency and biological safety of plant-derived nanoparticles. SPR of the studied AgNPs is observed at the wavelength of 425-430 nm, and the detection of biofunctional groups with the use of FTIR spectrometry is in agreement with previous research [29], where phenols and proteins were identified as efficient reducers and conductors that increased the stability of nanoparticles. From the present study's findings, AgNPs were proven to be more effective than the crude extract of pomegranate peel and precursor solution ($AgNO_3$) in combating *S. aureus and C. albicans*. This observation is in agreement with the findings of previous studies [30, 31], which reported a definite improvement in antimicrobial activities when nanoparticles having a high surface area were employed as their mode of penetration in microorganisms.

The MIC and MBC/MFC reported in the present study are not only consistent with the values found in the recent literature but at times surpass them. These findings are consistent with Díaz-Puertas et al. [32], who reported low and comparable MIC values for AgNPs synthesized using pomegranate peel extract. In addition, Khan et al. [33] demonstrated marked antibacterial activity of pomegranate peel-mediated AgNPs against *S. aureus*, supporting the antimicrobial effectiveness of biologically synthesized AgNPs. It was also consistent with the findings of research conducted in Iraq, where the antimicrobial potentials of AgNPs against *Pseudomonas aeruginosa* and *Staphylococcus aureus* were reported [14, 18]. The enhanced antimicrobial potential observed in this study may be attributed to the nanoscale morphology observed by TEM and the negative zeta potential value (-25 to -30 mV), which suggests initial electrostatic stabilization at the time of characterization rather than confirmed long-term colloidal stability. This surface charge may also facilitate interaction between AgNPs and microbial membranes.

Overall, the findings support the preliminary antimicrobial potential of pomegranate peel-mediated AgNPs under in vitro conditions. However, practical biomedical or formulation-related applications require further validation through cytotoxicity assessment, hemocompatibility testing, in vivo infection models, and storage stability evaluation. Although the use of agricultural by-products such as pomegranate peels may provide environmental and economic advantages, the current study should be interpreted as a preliminary synthesis and antimicrobial screening study rather than a formulation stability or shelf-life investigation.

3.4 Study scope and future perspectives

The present study focused on the green synthesis, physicochemical characterization, and in vitro antimicrobial evaluation of pomegranate peel-mediated AgNPs. The findings provide strong evidence for the successful formation of biologically synthesized AgNPs and demonstrate their promising antibacterial and antifungal activity against clinically relevant microbial isolates. The characterization results, including UV-Vis, FTIR, TEM, XRD, and zeta potential measurements, support the initial physicochemical profile of the synthesized nanoparticles at the time of analysis.

To further strengthen the translational and formulation-related potential of these nanoparticles, future studies should include a comprehensive storage stability assessment under controlled conditions. Such investigations would allow evaluation of possible changes in particle-size distribution, surface charge behavior, and antimicrobial activity over time. In addition, further biosafety assessments, including cytotoxicity, hemocompatibility, and in vivo infection models, would provide additional evidence supporting their potential biomedical applicability.

Elemental composition analysis by EDX was not performed in this study. Future work should include EDX analysis to confirm the purity and elemental composition of the synthesized nanoparticles.

4. CONCLUSION

The present study demonstrated the successful green synthesis of AgNPs using *Punica granatum* peel extract as a natural reducing and stabilizing agent. The formation of biologically synthesized AgNPs was supported by UV-Vis, FTIR, TEM, XRD, and zeta potential analyses, confirming the effective role of pomegranate peel phytoconstituents in nanoparticle formation and surface stabilization. The synthesized AgNPs exhibited notable antibacterial and antifungal activities against clinical isolates of *Staphylococcus aureus* and *Candida albicans*, with higher inhibition zones and favorable MIC, MBC, and MFC ranges compared with crude pomegranate peel extract and silver nitrate controls.

Overall, the findings highlight the potential of pomegranate peel-mediated AgNPs as eco-friendly antimicrobial nanomaterials and support the value of agricultural by-products in sustainable nanobiotechnology. To advance these nanoparticles toward broader biomedical or formulation-related applications, future investigations should include extended stability profiling under controlled storage conditions, with emphasis on particle-size distribution, surface charge behavior, and retention of antimicrobial activity over time. Additional biosafety evaluations, including cytotoxicity, hemocompatibility, and in vivo infection models, would further strengthen the translational relevance of the synthesized AgNPs.

REFERENCES

[1] World Health Organization. (2014). Antimicrobial Resistance: Global Report on Surveillance. World Health Organization. https://apps.who.int/iris/handle/10665/112642.

[2] Mohsin, A.S., Alsakini, A.H., Ali, M.R. (2022). Outbreak of drug resistance Escherichia coli phylogenetic F group associated urinary tract infection. Iranian Journal of Microbiology, 14(3): 341-350. https://doi.org/10.18502/ijm.v14i3.9771

[3] Turner, N.A., Sharma-Kuinkel, B.K., Maskarinec, S.A., et al. (2019). Methicillin-resistant Staphylococcus aureus: An overview of basic and clinical research. Nature Reviews Microbiology, 17(4): 203-218. https://doi.org/10.1038/s41579-018-0147-4

[4] Mohsin, A.S., Ali, M.R., Alsakini, A.H. (2026). Biofilm-associated genes and their role in antibiotic resistance among clinical Staphylococcus aureus isolates. Journal of Infection in Developing Countries, 20(3): 416-424. https://doi.org/10.3855/jidc.22026

[5] Calderone, R.A., Clancy, C.J. (2012). Candida and Candidiasis. 2nd ed. American Society for Microbiology Press.

[6] Aherkar, V.V., Mohammed, A.A., Al-Shimary, A.A., et al. (2025). Photocatalytic dye degradation efficacy and antimicrobial potency of zinc oxide nanoparticles synthesized via sol-gel method. Next Materials, 9: 100972. https://doi.org/10.1016/j.nxmate.2025.100972

[7] Aherkar, V., Mohammed, A.A., Al-Shimary, A.A., Ovhal, R.M., et al. (2026). Synthesis and characterization of Ag-doped ZnO nanostructures and an assessment on their enhanced bacterial inhibition and photocatalytic degradation. RSC Advances, 16(18): 16253-16263. https://doi.org/10.1039/D5RA09660J

[8] Gavali, L.V., Mohammed, A.A., Al-Ogaili, M.J., et al. (2024). Novel terephthalaldehyde bis(thiosemicarbazone) Schiff base ligand and its transition metal complexes as antibacterial agents: Synthesis, characterization and biological investigations. Results in Chemistry, 7: 101316. https://doi.org/10.1016/j.rechem.2024.101316

[9] Morones, J.R., Elechiguerra, J.L., Camacho, A., et al. (2005). The bactericidal effect of silver nanoparticles. Nanotechnology, 16(10): 2346-2353. https://doi.org/10.1088/0957-4484/16/10/059

[10] Dakal, T.C., Kumar, A., Majumdar, R.S., Yadav, V. (2016). Mechanistic basis of antimicrobial actions of silver nanoparticles. Frontiers in Microbiology, 7: 1831. https://doi.org/10.3389/fmicb.2016.01831

[11] Viuda-Martos, M., Fernández-López, J., Pérez-Álvarez, J.A. (2010). Pomegranate and its many functional components. Food Research International, 43(10): 2236-2247. https://doi.org/10.1016/j.foodres.2010.08.002

[12] Ismail, T., Sestili, P., Akhtar, S. (2012). Pomegranate peel and fruit extracts: A review of bioactive compounds and biological activities. Food Chemistry, 134(4): 2211-2223. https://doi.org/10.1016/j.foodchem.2012.02.006

[13] Mohsin, A.S., Alsakini, A.H., Ali, M.R. (2022). Molecular characterization of Dr/Afa genes prevalent among multi drug resistant Escherichia coli isolated from urinary tract infections. Biomedicine, 42(3): 523-529. https://doi.org/10.51248/.v42i3.1632

[14] Seror, A.A.H., Qadoori, S.S., Mohammed, T.K., Alabbas, A.S., Abdullah, H.N. (2020). Isolation of some pathogenic bacteria and Candida albicans from student accessories and watches as part of biosafety in medical laboratories. Biochemistry and Cell Archives, 20(2): 6565-6570.

[15] Al-Zoreky, N.S. (2009). Antimicrobial activity of pomegranate (Punica granatum L.) fruit peels. International Journal of Food Microbiology, 134(3): 244-248. https://doi.org/10.1016/j.ijfoodmicro.2009.07.002

[16] Jurenka, J. (2008). Therapeutic applications of pomegranate (Punica granatum L.): A review. Alternative Medicine Review, 13(2): 128-144.

[17] Mohammed, T.K., Jwad, M.A., Kamal, O., Abbas, A.H., Alabbas, A.S. (2019). Isolation of some pathogenic bacteria and fungi from student's mobile phones (Part I). Indian Journal of Public Health Research & Development, 10(10): 2108-2112. http://dx.doi.org/10.5958/0976-5506.2019.03162.0

[18] Anjum, S., Abbasi, B.H., Shinwari, Z.K. (2019). Green synthesis of silver nanoparticles using pomegranate peel extract and their antimicrobial activity. Materials Research Express, 6(4): 045045. https://doi.org/10.1088/2053-1591/aaf9b3

[19] Iravani, S. (2011). Green synthesis of metal nanoparticles using plants. Green Chemistry, 13(10): 2638-2650. https://doi.org/10.1039/C1GC15386B

[20] Zhang, X.F., Liu, Z.G., Shen, W., Gurunathan, S. (2016). Silver nanoparticles: Synthesis, characterization, properties, applications, and therapeutic approaches. International Journal of Molecular Sciences, 17(9): 1534. https://doi.org/10.3390/ijms17091534

[21] Ahmed, S., Ahmad, M., Swami, B.L., Ikram, S. (2016). Green synthesis of silver nanoparticles using plant extracts. Journal of Advanced Research, 7(1): 17-28. https://doi.org/10.1016/j.jare.2015.02.021

[22] Singh, P., Kim, Y.J., Zhang, D., Yang, D.C. (2016). Biological synthesis of nanoparticles from plants and microorganisms. Biotechnology Advances, 34(4): 588-599. https://doi.org/10.1016/j.biotechadv.2016.02.006

[23] Mohammed, T.K., Aqel, N., Al-Dujaili, E.A.S. (2020). Antimicrobial activity of liquid residues of Cymbopogon citratus oil extracts. Journal of Physics: Conference Series, 1660: 012006. https://doi.org/10.1088/1742-6596/1660/1/012006

[24] Abdel-Rahman, L.H., Abu-Dief, A.M., Hashem, N.A. (2019). Antibacterial and antifungal activities of green silver nanoparticles against Staphylococcus aureus and Candida albicans. Journal of Inorganic and Organometallic Polymers and Materials, 29: 831-840. https://doi.org/10.1007/s10904-019-01083-6

[25] Abbas, Z.N., Hanaa, N.A., Zahra, H., Bijan, R. (2024). Antibacterial and antibiofilm activity of zinc oxide quantum dots against methicillin-resistant Staphylococcus aureus. Particle & Particle Systems Characterization, 41(12): 2400048. https://doi.org/10.1002/ppsc.202400048

[26] Mostafa, Y.S., Alamri, S.A., Alrumman, S.A., Hashem, M., Baka, Z.A. (2021). Green synthesis of silver nanoparticles using pomegranate peel extract and their antifungal activity against Alternaria solani, the causal agent of early blight disease of tomato. Plants, 10(11): 2363. https://doi.org/10.3390/plants10112363

[27] Farouk, S.M., Abu-Hussien, S.H., Abd-Elhalim, B.T., et al. (2023). Biosynthesis and characterization of silver

nanoparticles from Punica granatum (pomegranate) peel waste and its application to inhibit foodborne pathogens. Scientific Reports, 13(1): 19469. https://doi.org/10.1038/s41598-023-46355-x

[28] Sari Gencag, B., Kahraman, K., Ekici, L. (2025). Green synthesis of silver nanoparticles from pomegranate peel and their application in PVA-based nanofibers for coating minced meat. Scientific Reports, 15: 17083. https://doi.org/10.1038/s41598-025-95349-4

[29] Saad, P.G., Castelino, R.D., Ravi, V., Al-Amri, I.S., Khan, S.A. (2021). Green synthesis of silver nanoparticles using Omani pomegranate peel extract and two polyphenolic natural products: Characterization and comparison of their antioxidant, antibacterial, and cytotoxic activities. Beni-Suef University Journal of Basic and Applied Sciences, 10: 29. https://doi.org/10.1186/s43088-021-00119-6

[30] Fernandes, R.A., Berretta, A.A., Torres, E.C., et al. (2018). Antimicrobial potential and cytotoxicity of silver nanoparticles phytosynthesized by pomegranate peel extract. Antibiotics, 7(3): 51. https://doi.org/10.3390/antibiotics7030051

[31] Devanesan, S., AlSalhi, M. S., Balaji, R.V., et al. (2018). Antimicrobial and cytotoxicity effects of synthesized silver nanoparticles from Punica granatum peel extract. Nanoscale Research Letters, 13(1): 315. https://doi.org/10.1186/s11671-018-2731-y

[32] Díaz-Puertas, R., Álvarez-Martínez, F.J., Rodríguez-Cañas, E., et al. (2025). An innovative approach based on the green synthesis of silver nanoparticles using pomegranate peel extract for antibacterial purposes. Bioinorganic Chemistry and Applications, 2025: 2009069. https://doi.org/10.1155/bca/2009069

[33] Khan, A.A., Alanazi, A.M., Alsaif, N., Wani, T.A., Bhat, M.A. (2021). Pomegranate peel induced biogenic synthesis of silver nanoparticles and their multifaceted potential against intracellular pathogens and cancer. Saudi Journal of Biological Sciences, 28(8): 4191-4200. https://doi.org/10.1016/j.sjbs.2021.06.022